Activation of CO_2 at Chromia-Nanocluster-Modified Rutile and Anatase TiO_2

Michael Nolan[1]* and Marco Fronzi[1,2]

1: Tyndall National Institute, University College Cork, Lee Maltings, Prospect Row, Cork, T12 R5CP, Ireland

2: International Research Centre for Renewable Energy, State Key Laboratory of Multiphase Flow in Power Engineering, Xi'an Jiaotong University, Xi'an 710049, Shaanxi, China.

*michael.nolan@tyndall.ie

Abstract

Converting CO_2 to fuels is required to enable the production of sustainable fuels and to contribute to alleviating CO_2 emissions. In considering conversion of CO_2, the initial step of adsorption and activation by the catalyst is crucial. In addressing this difficult problem, we have examined how nanoclusters of reducible metal oxides supported on TiO_2 can promote CO_2 activation. In this paper we present density functional theory (DFT) simulations of CO_2 activation on heterostructures composed of clean or hydroxylated extended rutile and anatase TiO_2 surfaces modified with chromia nanoclusters. The heterostructures show non-bulk Cr and O sites in the nanoclusters and an upshifted valence band edge that is dominated by Cr 3d- O 2p interactions. We show that the supported chromia nanoclusters can adsorb and activate CO_2 and that activation of CO_2 is promoted whether the TiO_2 support is oxidised or

hydroxylated. Reduced heterostructures, formed by removal of oxygen from the chromia nanocluster, also promote CO_2 activation. In the strong CO_2 adsorption modes, the molecule bends giving O-C-O angles of 127 - 132° and elongation of C-O distances up to 1.30 Å; no carbonates are formed. The electronic properties show a strong CO_2-Cr-O interaction that drives the interaction of CO_2 with the nanocluster and induces the structural distortions. These results highlight that a metal oxide support modified with reducible metal oxide nanoclusters can activate CO_2, thus helping to overcome difficulties associated with the difficult first step in CO_2 conversion.

Keywords: DFT; CO_2 activation; adsorption; heterostructures

1. Introduction

CO_2 emissions from fossil fuels are the major cause of climate change and need to be eliminated in the near future to meet the targets of the COP21 Paris agreement to keep average global temperature increases below 2°C. Thus finding solutions to remove and store or use this CO_2 is a key concern. A solar driven photo- or thermochemical process for the conversion of CO_2 to CO, coupled with solar water splitting can produce synthesis gas, while direct conversion of CO_2 to liquid fuels would enable a sustainable approach to producing fuels and storing solar energy in high energy chemical bonds[1-11].

However, CO_2, as the most oxidised form of carbon, is highly stable and therefore activating it as part of the conversion process is difficult. In fact, to date, there are no widely available catalysts that can exploit solar energy (either directly or via thermochemical processes) to efficiently reduce CO_2 to useful chemicals. One successful example of a photocatalyst has been Pt-modified TiO_2 nanotubes[8, 12, 13] that produce methane. However, the efficiencies for

methane production are extremely low and Pt will never be an economically viable catalyst for large scale CO_2 conversion.

Copper has been shown to promote conversion of CO_2 into hydrocarbons, while many other metallic catalysts promote hydrogen evolution. More recently, catalysts based on oxide-derived Cu or Cu with mixed oxidation states have been shown to reduce CO_2 to useful molecules such as methane, methanol or ethanol [2, 14-26]. While this is encouraging, there is still an urgent need from a fundamental perspective to understand the factors that drive CO_2 activation and find materials to promote this process. Since a CO_2 anion ($CO_2^{\delta-}$) is implicated in CO_2 conversion, using materials with excess electrons is one path to the development of CO_2 activation catalysts. These electrons could be produced through light excitation or formation of oxygen vacancies which release electrons to the catalyst. Transition metal-oxide based catalysts could show some promise in this regard; the work on Cu-based catalysts suggests a pathway towards exploiting reducible metal oxides for CO_2 conversion. It is also possible to promote CO_2 activation without necessarily producing an anionic species and this would be driven by interactions at suitable sites in the catalyst and/or suitable energy level alignments of the catalyst and CO_2.

Irrespective of the origin of the electrons that reduce CO_2, in any CO_2 conversion process the initial adsorption and activation of CO_2 is a key step. Thereafter there may be transfer of electron(s) to the CO_2 through light absorption or from excess electrons present in the catalyst after catalyst (pre-)reduction or in a combined PV+electrolysis system. Thus, the key challenge in fuel production from CO_2 is to discover catalysts that will promote the crucial first step, namely the adsorption and activation of CO_2.

Copper-based catalysts have been widely studied for CO_2 activation and conversion and this includes Cu metal, oxide-derived Cu and mixed oxidation state Cu [2, 14-26]. Modelling the

interaction of CO_2 with copper oxides uses density functional theory (DFT) to provide insights for further development of CO_2 activation catalysts. Wu *et al.* studied the adsorption of CO_2 at the Cu_2O (111) surface with oxygen vacancies [17], and found that dissociative adsorption was thermodynamically unfeasible. In addition, while a $CO_2^{\delta-}$ radical anion species can form on a defective surface, this is not stable. Wu *et al.* examined at the adsorption of CO_2 at Cu_2O (111) using Hybrid DFT [21] and found adsorption only in non-activated form. This was confirmed by Bendavid and Carter [18]. Mishra *et al.* found similar results for CO_2 adsorption at Cu_2O (111), but reported strong chemisorption at the high energy Cu-O terminated (110) surface[14] and at the (011) surface of CuO [2]. Uzunova *et al.* studied the conversion of CO_2 to methanol on Cu_2O nanolayers and clusters [16] using Hybrid DFT. In the work of Favaro *et al.*[24] a model of Cu with subsurface oxygen was found to activate CO_2.

The adsorption of CO_2 molecules at different titania surfaces, including rutile and anatase, and nanostructures has also been well studied and the role of low coordinated sites, surface structure and oxygen vacancies has been discussed [27-32]. The presence of excess electrons and holes was shown to drive adsorption and activation of CO_2 at rutile (110) [33]. Yang *et al.* showed that sub-nm Pt clusters at the anatase (101) surface enhanced CO_2 activation through providing of additional adsorption sites and the transfer of electron density to the TiO_2 substrate [34]. Fewer studies exist for other metal oxide systems, but some examples include Cu/CeO_2 and $Cu/CeO_2/TiO_2$ [35], $Cu/ZnO/Al_2O_3$ [36] and dispersed CeO_2/TiO_2 [37]; the role of Ce^{3+} in visible light absorption, photogenerated charge separation and strengthening CO_2-surface bonding was highlighted.

Previously we have used first principles density functional theory (DFT) simulations to study heterostructured materials composed of TiO_2 (rutile or anatase) modified with metal oxide nanoclusters. In earlier work, the emphasis focussed on systems with predicted visible light absorption[38-49] and reduced charge recombination[39-43, 50, 51]. We have begun to extend

this work to study the interaction of molecules, such as CO_2, with these metal oxide nanocluster modified TiO_2 systems [38, 52]. We have investigated modified TiO_2 systems, *e.g.* ZrO_2-anatase, where CO_2 can adsorb and be activated [38] and reduced MnO_x-TiO_2 which show weak or unfavourable interactions with CO_2 [52]. There is therefore still much work to be done to understand the factors that drive CO_2 activation on metal oxides.

In the present paper, we use first principles density functional theory to examine in detail the interaction and activation of CO_2 at Cr_2O_3 nanocluster modified rutile and anatase TiO_2 surfaces, which are oxidised or hydroxylated. The interaction of CO_2 with reduced Cr_2O_3-TiO_2 heterostructures, upon loss of oxygen from the nanocluster, is also examined. While chromia is by far less studied for CO_2 adsorption compared to other oxides, there have a number of experimental surface science studies devoted to this topic [53-57]. These have discussed difficulties in obtaining high quality films of chromia or single crystals of Cr metal. Thus, chromia grown through oxidation of metallic Cr or chromia micropowders have been employed. These studies use infra red (IR) spectroscopy and thermal desorption spectroscopy (TDS) to examine the role of the termination of the chromia film on CO_2 adsorption. Termination with Cr enables strong adsorption of CO_2, as determined from TDS, with formation of carboxylate or carbonates. Termination with chromyl oxygen can bury these Cr sites and facilitates physisorption of linear CO_2, with a lower temperature TDS peak. The IR spectra show clear differences between the CO_2 adsorption modes. We find that chromia modified TiO_2 heterostructures are able to activate CO_2, causing O-C-O bending and elongation of C-O distances. This is independent of the state or identity of the TiO_2 surface, indicating that chromia nanoclusters drive CO_2 activation. In addition, reduced Cr_2O_3-TiO_2 heterostructures also activate CO_2. These findings thus show that transition metal oxide nanocluster modification of rutile and anatase TiO_2 produces heterostructures that can activate CO_2.

2. Methods

Following our approach from previous work on chromia-modified rutile and anatase[58] we prepare heterostructures of nanoclusters with Cr_4O_6 stoichiometry supported on rutile (110) and anatase (101); the Supporting Information contains full details. We use a three dimensional periodic surface slab within VASP [59-62], and a plane wave basis set. Projector augmented wave potentials[63, 64], with 4, 12, 6, 4 and 1 valence electrons for Ti, Cr, O, C and H are used [58]. The cut-off for the kinetic energy is 396 eV and the exchange-correlation functional is the Perdew-Wang 91[65] approximation. A Monkhorst-Pack (2×1×1) **k**-point sampling grid is used. We apply the DFT+U approach [66] to describe the Ti 3d and Cr 3d states, with U = 4.5 eV for the Ti 3d states and 3.5 eV for the Cr 3d states [67, 68]. This DFT+U set-up is designed to recover a consistent description of the localisation of electrons in reduced cations rather than to recover the band gap. Convergence criteria for electronic and ionic relaxations are 0.0001 eV and 0.02 eV/ Å. All calculations are spin polarised.

(2x4) and (4x2) surface supercell expansions are employed for rutile and anatase, respectively and the vacuum gap in all cases is 12 Å. The TiO_2 surfaces are unmodified oxidised or hydroxylated rutile (110) and anatase (101) surfaces [40, 58]. The free chromia nanoclusters are relaxed within the same computational described above, starting from different atomic arrangements. The most stable atomic structure of the free chromia Cr_4O_6 nanocluster is then adsorbed on the oxidised and hydroxylated TiO_2 surfaces in different adsorption configurations and these are relaxed. We then use the most stable relaxed chromia-TiO_2 heterostructures for subsequent study with CO_2 [39, 48, 51]. When clean rutile is modified with Cr_4O_6, this is denoted **Cr_4O_6-o-rutile** and when hydroxylated rutile is modified with Cr_4O_6, this is denoted **Cr_4O_6-oh-rutile**; a similar nomenclature is used for anatase. The term **Cr_2O_3-TiO_2** indicates a

non-specific Cr_2O_3 nanocluster-modified TiO_2 heterostructure. Although the detailed study of the interaction of water at chromia-TiO_2 heterostructures is beyond the scope of this work, we have found that adsorption of water at Cr_4O_6-o-rutile and Cr_4O_6-oh-rutile is molecular with adsorption energies of -0.3 and -0.8 eV, so that there is a barrier to hydroxyl formation on adsorbed chromia.

The stability of the heterostructure is characterised by the nanocluster adsorption energy, E^{ads}

$$E^{ads} = E[(Cr_4O_6)\text{-}TiO_2] - \{E[(Cr_4O_6)] + E[TiO_2]\} \quad (1)$$

Where $E[(Cr_4O_6)\text{-}TiO_2]$ is the computed total energy of Cr_4O_6 nanocluster-modified TiO_2, $E(Cr_4O_6)$ is the computed total energy of the free Cr_4O_6 nanocluster and $E(TiO_2)$ is the computed total energy of the unmodified TiO_2 (rutile/anatase) surface.

The CO_2 adsorption energy is defined in Eqn (2):

$$E^{ads} = E[CO_2@Cr_4O_6\text{-}TiO_2] - \{E[Cr_4O_6\text{-}TiO_2] + E[CO_2]\} \quad (2)$$

where $E[CO_2@Cr_4O_6\text{-}TiO_2]$ is the computed total energy of CO_2 adsorbed at Cr_4O_6-modified TiO_2.

3. Results

We first briefly summarise the atomic structure of chromia-modified rutile and anatase TiO_2, in which the TiO_2 supports are oxidised or hydroxylated ½ ML coverage. These are shown in **Figures S1** and **S2** of the supporting information. Adsorption and relaxation of Cr_4O_6 on both TiO_2 surfaces gives adsorption energies of -4.25 eV and -5.85 eV on oxidised rutile and anatase and -1.08 eV and -2.21 eV on hydroxylated rutile and anatase, indicating strong nanocluster-surface interactions. The presence of surface hydroxyls and the migration of hydrogen to the support nanocluster reduce the energy gain upon chromia adsorption at hydroxylated surfaces.

Ti and Cr sites have the expected +4 and +3 oxidation states. Exceptions to this are Cr_4O_6-o-anatase, where a reduced Ti^{3+} and an oxidised Cr^{4+} cation are formed, and Cr_4O_6-oh-anatase, where 2 Cr^{2+} and 2 Cr^{4+} cations are present. In all heterostructures, the valence band edge is modified by the adsorption of Cr_4O_6 pushing the VB edge to higher energy. Oxygen vacancies can form readily in these systems, with formation energies of 0.22 eV and 1.95 eV on Cr_4O_6-o-rutile and Cr_4O_6-o-anatase, while these formation energies are 0.69 eV and 0.35 eV on Cr_4O_6-oh-rutile and Cr_4O_6-oh-anatase. Upon reduction, heterostructures of chromia on oxidised and hydroxylated supports show the presence of reduced Ti^{3+} and Cr^{2+} species.

3.1 Adsorption and Activation of CO_2 at Chromia-Modified Rutile (110) and Anatase (101)

3.1.1 CO_2 Adsorption at Cr_4O_6-modified rutile

Figure 1 shows the atomic structure for the two most stable CO_2 adsorption modes that we have found at Cr_4O_6-o-rutile (110) (Figure 1(a), (b)), modes I and II) and Cr_4O_6-oh-rutile (110) (Figure 1(c), (d) modes I and II). The computed adsorption energies for the two CO_2 adsorption modes on Cr_4O_6-o-rutile (110) are -0.63 eV and -0.91 eV for modes I and II. In Cr_4O_6-oh-rutile (110), the CO_2 adsorption energies are -0.92 eV and -0.31 eV for modes I and II. Clearly the modification of rutile with chromia produces heterostructures that show moderately strong adsorption capability for CO_2, which is the first requirement for CO_2 conversion. These energies are 0 K DFT energy differences and if we include the zero point energy corrections (ZPE) for CO_2 adsorption these are only on the order of 0.03 eV which makes no significant change to the adsorption energies at chromia-modified TiO_2. If we compare with the available

work on CO_2 adsorption at chromia, then the moderately strong adsorption energies can arise from the availability of Cr sites in the nanocluster to interact with oxygen of CO_2, in a similar to the stronger Cr-CO_2 interaction described experimentally in refs[54-56].

We have examined multiple CO_2 adsorption sites on each chromia-TiO_2 system and other, less favourable adsorption modes are shown in Figures S3 and S4 and the energies relative to the most stable adsorption mode are shown in Table S1 of the Supporting Information. Even though these adsorption modes are less stable than those shown in Figure 1, we can see that they still generally show moderate CO_2 adsorption energies and similar adsorption structures, so that CO_2 adsorption and activation at multiple sites of chromia-modified TiO_2 is likely. We have also relaxed the adsorption structures in Figure 1 with no +U correction and find that the adsorption of CO_2 and the changes to its geometry are not influenced by the inclusion of the +U correction into the computational set-up.

In discussing the adsorption structure of CO_2, we focus on the change in molecular C-O distances and the O-C-O angle. In gas phase CO_2, the C-O distances are 1.16 Å, while the O-C-O angle is 180º. On Cr_4O_6-o-rutile, CO_2 adsorption in mode I results in the C-O distances elongating to 1.27 and 1.23 Å, while the O-C-O angle is 132º. One oxygen atom of CO_2 binds to a Cr site in the nanocluster, with a Cr-O distance of 2.05 Å. Finally, the C-O distance to the nanocluster is 1.44 Å. In adsorption mode II, the C-O distances in adsorbed CO_2 both lengthen to 1.27 Å and the O-C-O angle is 130º. Both oxygen atoms of the molecule bind to Cr sites in the nanocluster, with Cr-O distances of 2.08 Å and 2.13 Å. The carbon of CO_2 shows a C-O distance to the nanocluster of 1.39 Å. Thus, the adsorption of CO_2 causes a lengthening of molecular C-O distances and bending of the molecule, characteristic of CO_2 activation [4, 69]. We also note that the deviation from linearity in the O-C-O angle increases with the strength of CO_2 adsorption.

Finally, we have computed the vibrational frequencies of adsorbed CO_2; for reference our computed vibrational modes for gas-phase CO_2 are 2354, 1325, and 632 cm^{-1} and the experimental CO_2 vibrational modes are 2349, 1333 and 667 cm^{-1} [70] so that our gas phase CO_2 vibrational modes are in good agreement with experiment. In mode I, the computed vibrational modes are 1720, 1221, 791 and 767 cm^{-1}, while in mode II, the vibrational modes are 1589, 1226, 921 and 803 cm^{-1}. We note the large red shift of up to 765 cm^{-1} in the C=O stretching mode and the lifting of the degeneracy of the O-C-O bending mode upon adsorption of CO_2 on the chromia nanocluster. The C-O elongation is not as large in mode I so the shift in the C=O stretching mode is correspondingly smaller. These results strongly indicate that CO_2 adsorbs in an activated mode.

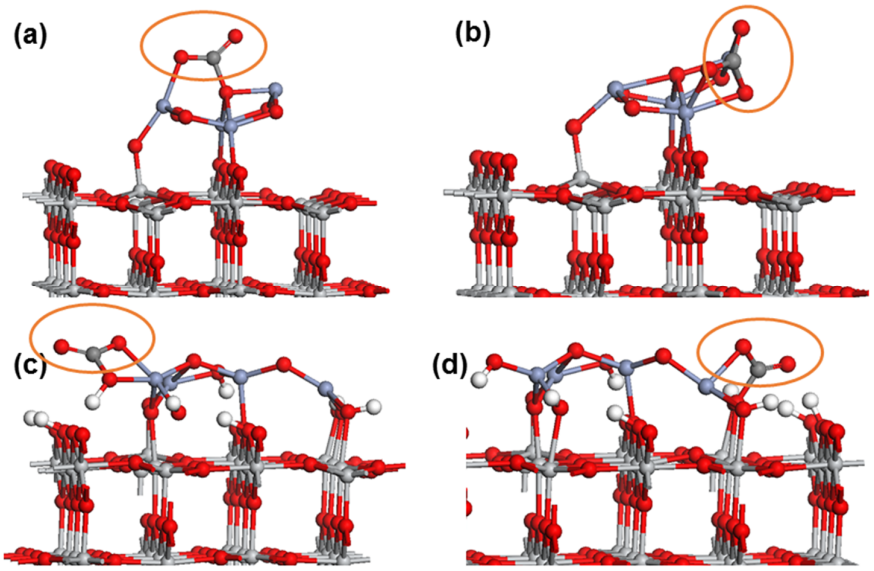

Figure 1: Relaxed atomic structures for CO_2 adsorbed in two adsorption modes at **(a), (b)** Cr_4O_6-o-rutile and **(c), (d)** Cr_4O_6-oh-rutile. The colour scheme is Ti: grey spheres, O: red spheres, Cr: blue spheres and C: grey spheres. The ring shows the CO_2 molecule.

If we turn to activation of CO_2 at the Cr_4O_6-oh-rutile (110) heterostructure, adsorption of CO_2 in mode I (Figure 1(c)) results in an elongation of the molecular C-O distances to 1.21 and 1.31 Å, while the O-C-O angle is bent, with an angle of 132°. The C-O distance to the nanocluster is 1.44 Å and the Cr-O distance to the molecule is 1.99 Å. In adsorption mode II (Figure 1(d)), the C-O distances are 1.24 and 1.30 Å, while the O-C-O angle is 128°. We note the stronger elongation of one C-O distance upon adsorption at Cr_4O_6-oh-rutile compared to adsorption at Cr_4O_6-o-rutile. The oxygen involved is bound to Cr in the nanocluster, so this extra interaction permits a lengthening of the C-O bond.

The computed vibrational modes are 1774, 1152, 899, 796 cm^{-1} and 1658, 1206, 927 and 772 cm^{-1} for modes I and II, respectively. These are similar to CO_2 adsorption at the Cr_4O_6-o-rutile heterostructure and the non-uniform elongation of the C-O distances results in a smaller red shift in the C=O stretching mode. Thus, the interaction of CO_2 at chromia-modified rutile results in strong adsorption and activation of the molecule and this is irrespective of the state of the support. The activation of CO_2 is accompanied by distortions to the molecule, namely C-O bond elongation and O-C-O bending.

3.1.2 CO_2 Adsorption at Cr_4O_6-modified anatase

Figure 2 shows the atomic structure for two CO_2 adsorption modes at Cr_4O_6-o-anatase (101) (Figure 2(a), (b)), modes I and II) and Cr_4O_6-oh-anatase (101) (Figure 2(c), (d) modes I and II). On Cr_4O_6-o-anatase (101), adsorption of CO_2 in mode I has a rather large adsorption energy of -2 eV, suggesting that the CO_2 may be overstabilised upon adsorption. In mode II, the computed adsorption energy is -0.13 eV. However, we note for adsorption mode II that a CO molecule is directly formed and this process is exothermic. The C-O distance in the free CO molecule is 1.14 Å.

In adsorption mode I, the C-O distances elongate to 1.26 and 1.28 Å and the O-C-O angle is 133º. The C-O distance to the nanocluster is 1.39 Å and the Cr-O distance to the molecule is 2.13 Å. Computed vibrational modes of adsorbed CO_2 in mode I are 1617, 1201, 915 and 906 cm^{-1}, which again show activation of adsorbed CO_2.

After CO_2 adsorption on Cr_4O_6-oh-anatase (101), the computed adsorption energies are -0.71 eV and -1.11 eV for modes I and II, respectively. In a similar fashion to the results on chromia-rutile, the availability of Cr sites in the nanocluster permits interaction with CO_2. In mode I the molecular C-O distances are 1.25 and 1.28 Å, with an O-C-O bending angle of 127º. In mode II, the C-O distances are 1.24 and 1.29 Å and the O-C-O bending angle is 128º. Computed vibrational modes for adsorbed CO_2 are 1628, 1246, 908 and 799 cm^{-1} on Cr_4O_6-o-anatase and 1642, 1243, 959 and 777 cm^{-1} on Cr_4O_6-oh-anatase. Thus, the activation of CO_2 at chromia modified anatase is not dependence on the state of the TiO_2 support.

We recall that Cr_4O_6-o-anatase has a reduced Ti^{3+} and a Cr^{4+} cation [58]. Upon formation of activated CO_2 (mode I), both cations are partially reoxidised and there is a charge redistribution, with a transfer of 0.5 electrons to CO_2. Upon formation of CO, examination of the computed indicates reoxidation of the Cr^{2+} and Ti^{3+}, with a transfer of 2 electrons to adsorbed CO_2 which promotes the formation of CO.

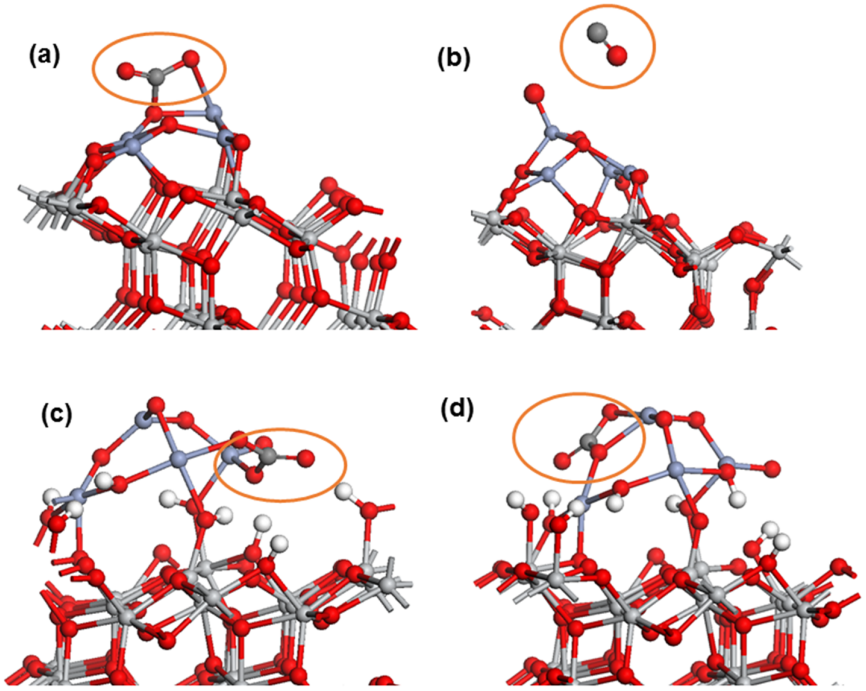

Figure 2: Relaxed atomic structures for CO_2 adsorbed in two adsorption modes at **(a), (b)** Cr_4O_6-o-anatase and **(c), (d)** Cr_4O_6-oh-anatase. The colour scheme is the same as Figure 1. The ring shows the CO_2 molecule.

3.2 Adsorption and Activation of CO_2 at Reduced Chromia-Modified Rutile and Anatase

We finally consider the adsorption of CO_2 at two examples of reduced Cr_2O_3-TiO_2, where the rutile and anatase supports are hydroxylated. Since in any process for conversion of CO_2, water is likely to be used as a proton source, the supports will most likely have some coverage of water present and this is accounted for by using our ½ ML hydroxylated supports. In addition, the reduction energies of chromia-modified hydroxylated TiO_2 are moderate, so this needs to be taken into account when investigating CO_2 activation.

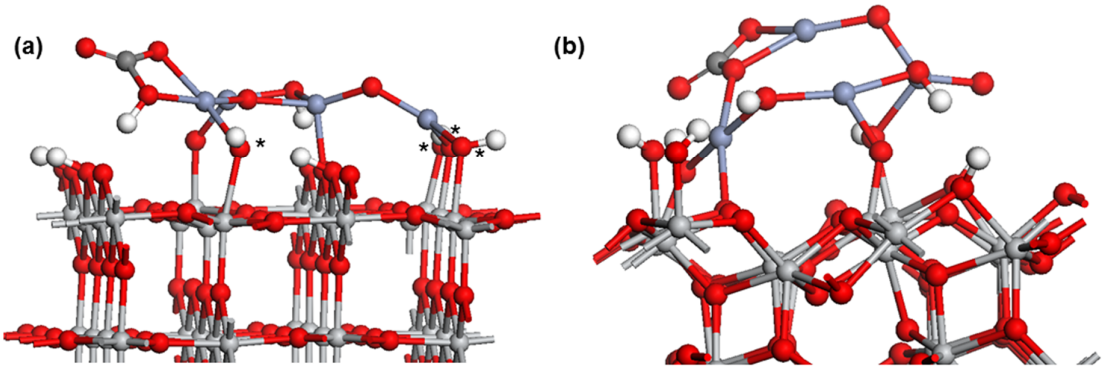

Figure 3: Relaxed atomic structures for CO_2 adsorbed at **(a)** reduced Cr_4O_5-oh-rutile and **(b)** reduced Cr_4O_5-oh-anatase. The colour scheme is the same as Figure 1.

Figure 3 shows the atomic structure of CO_2 adsorbed at reduced Cr_4O_5-oh-rutile (110) and Cr_4O_5-oh-anatase (101). The computed CO_2 adsorption energies are -0.6 eV and -1.85 eV on rutile and anatase, respectively. The presence of the oxygen vacancy in the chromia nanocluster promotes adsorption of CO_2, particularly on the anatase support. Hydrogen atoms from the hydroxyl sites do not migrate to the adsorbed CO_2.

The C-O distances in the molecule elongate to 1.21 and 1.29 Å upon adsorption at Cr_4O_5-oh-rutile and to 1.24 and 1.31 Å upon adsorption at Cr_4O_5-oh-anatase. The corresponding O-C-O angles are 133º (rutile) and 127º (anatase). The third C-O distance to the nanocluster is 1.47 and 1.37 Å in Cr_4O_5-oh-rutile and Cr_4O_5-oh-anatase.

When we examine the oxidation states of the Ti and Cr cations in the supports and the nanocluster, the adsorption of CO_2 does not result in any significant change in the oxidation states of Ti and Cr cations; such changes are on the order of < 0.1 electrons so that reduced cation species persist. Thus, we suggest that there is some charge redistribution upon bonding with CO_2.

4. Discussion and Conclusion

Finding materials that can activate CO_2 is of high interest for using CO_2 as a feedstock for sustainable fuel production. The present study shows that CO_2 can adsorb and activate at chromia nanocluster modified rutile and anatase TiO_2 heterostructures. We characterise the activation of CO_2 by the strength of adsorption, the elongation of C-O distances, the bending of the O-C-O angle and the red shift in the C=O stretching mode. In almost all cases we find moderately strong CO_2 adsorption; the exception is at Cr_4O_6-o-anatase. The C-O distances elongate, with a particularly strong elongation on chromia-anatase heterostructures, where the C-O distances elongate up to 1.30 Å. On chromia-rutile, the elongation is not uniform, with one C-O bond clearly longer than the other. The O-C-O angle always shows significant bending, where we find angles in the range of 127 – 132°. The state of the TiO_2 support, whether perfect or hydroxylated, and reduction of the chromia nanocluster, do not influence the adsorption and activation of CO_2 and it is therefore the chromia nanocluster modifier that promotes CO_2 adsorption.

The supported nanoclusters offer some advantageous properties for CO_2 activation. Firstly, there are low coordinated metal and oxygen sites in such non-bulk like structures, which have the potential to be active towards molecular adsorption. Secondly the presence of non-bulk like atomic environments can modify the electronic structure relative to bulk materials and the support. To examine any electronic structure effects, we show the projected electronic density of states (PEDOS) for the examples of CO_2 adsorption in mode I on C_4O_6-oh-rutile and in mode I on Cr_4O_6-oh-anatase in Figures 4 and 5. We recall that in the heterostructures, there are Cr_4O_6-derived electronic states above the valence band edge of the TiO_2 support. The PEDOS show

that these states persist upon adsorption of CO_2. Importantly, the CO_2 PEDOS, decomposed into C 2p and O 2p contributions, shows broad PEDOS peaks which are indicative of strong interactions between CO_2 and the oxide nanocluster. In particular, the O 2p states are found in the same energy range as the Cr_4O_6 states, while the C 2p PEDOS is also broad in the region from -2 eV to -6 eV below the highest occupied states. Thus, it is clear that the position of the Cr_4O_6-TiO_2 electronic states is suitable to allow hybridisation with the C 2p and O 2p states of CO_2. We note also that some supported chromia nanoclusters have Cr^{2+} oxidation states, and reducing the heterostructure through oxygen removal produces Ti^{3+} and Cr^{2+} sites. After adsorption of CO_2, we find that there can be reoxidation of these reduced cations, particularly in the case of CO formation, in which electron transfer from reduced Ti and Cr species is found. In other cases there is a redistribution of charge upon CO_2 adsorption. Thus, the chromia-modified TiO_2 heterostructures display suitable characteristics, namely active sites, suitable energy level positions and variable cation oxidation states which promote the adsorption and activation of CO_2.

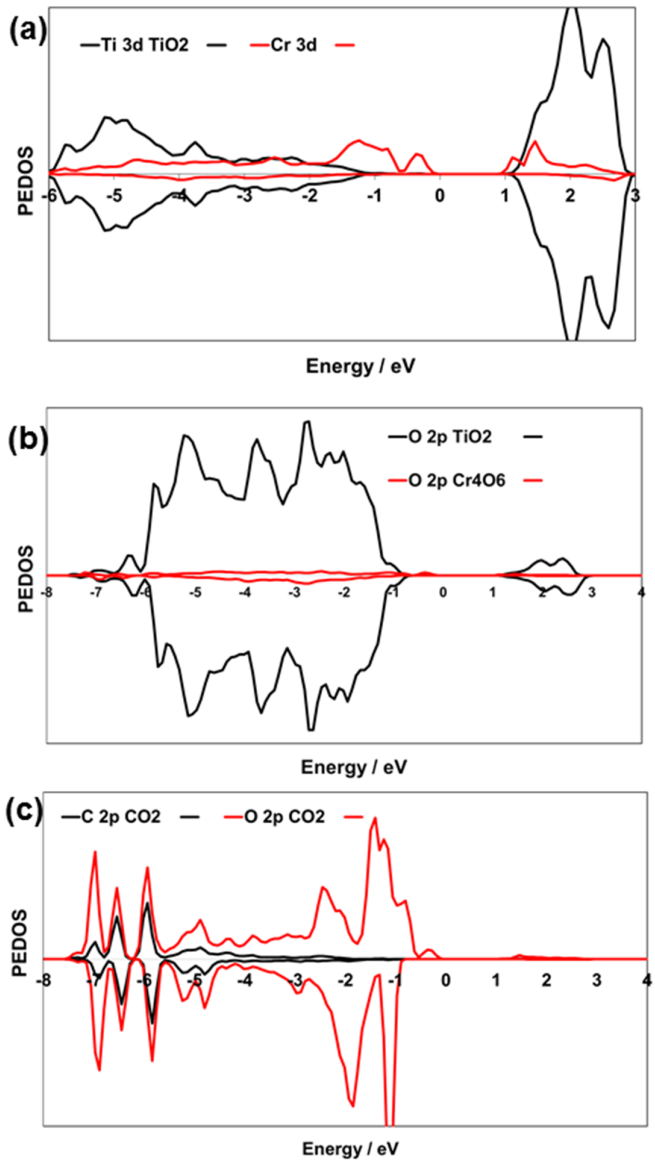

Figure 4: Projected electronic density of states for CO_2 adsorbed on Cr_4O_6-oh-rutile (110). The PEDOS is shown for Cr 3d and O 2p states in chromia, Ti 3d and O 2p states in TiO_2 and C and O 2p states in adsorbed CO_2. The zero of energy is the top of the highest occupied states.

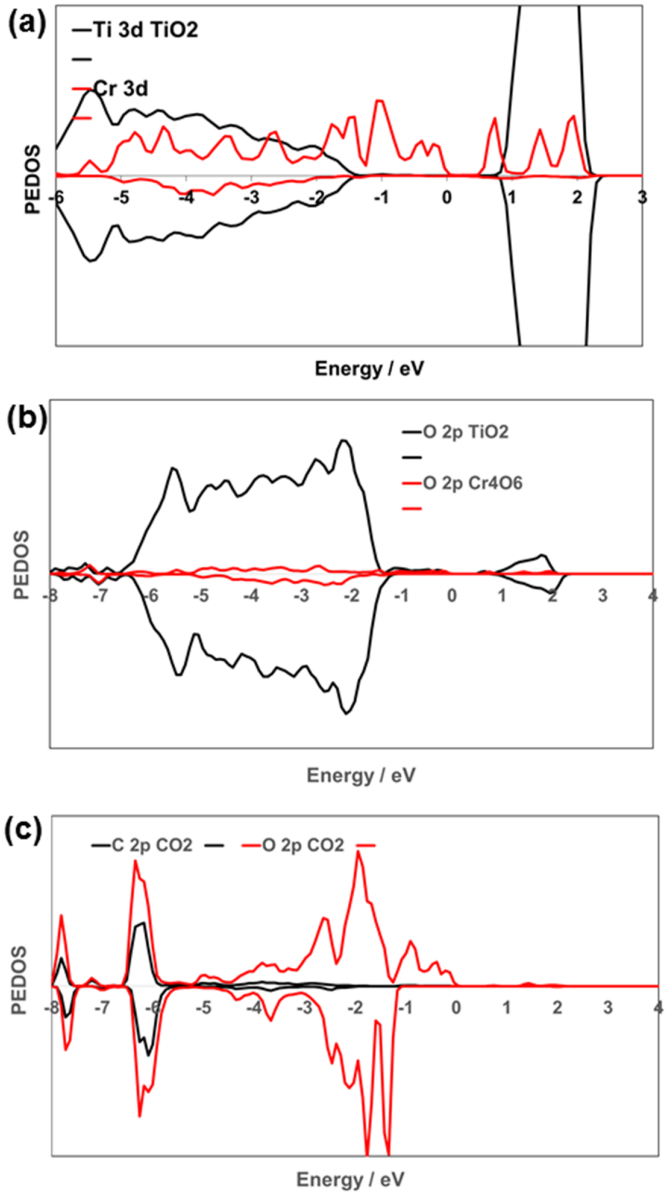

Figure 5: Projected electronic density of states for CO_2 adsorbed on Cr_4O_6-oh-anatase (110). The PEDOS is shown for Cr 3d and O 2p states in chromia, Ti 3d and O 2p states in TiO_2 and C and O 2p states in adsorbed CO_2. The zero of energy is the top of the highest occupied states.

In conclusion, the results of DFT studies of CO_2 adsorption at chromia-modified rutile and anatase TiO_2 surfaces show that these heterostructures are able to adsorb and activate CO_2, thus contributing to expanding the range of oxide-based structures that can promote the critical first step in the conversion of CO_2.

Acknowledgements

We acknowledge support from Science Foundation Ireland through the US-Ireland R&D Partnership Program Project SusChem SFI 14/US/E2915 and the M-ERA.net co-fund program, grant number SFI 16/M-ERA/2918, H2020 Grant Agreement 685451. Access to the computational resources at the Science Foundation Ireland/Higher Education Authority funded Irish Centre for High End Computing is acknowledged.

References

[1] X. Chang, T. Wang, J. Gong, CO_2 photo-reduction: insights into CO_2 activation and reaction on surfaces of photocatalysts, Energy Environ Sci., 9 (2016) 2177-2196.
[2] A.K. Mishra, A. Roldán, N.H. de Leeuw, CuO Surfaces and CO_2 Activation: A Dispersion-Corrected DFT+U Study, J. Phys. Chem. C, 120 (2016) 2198-2214.
[3] S. Kwon, P. Liao, P.C. Stair, R.Q. Snurr, Alkaline-earth metal-oxide overlayers on TiO_2: application toward CO2 photoreduction, Catal. Sci. Technol., 6 (2016) 7885-7895.
[4] C. Kunkel, F. Viñes, F. Illas, Transition metal carbides as novel materials for CO_2 capture, storage, and activation, Energy Environ Sci., 9 (2016) 141-144.
[5] C. Peng, G. Reid, H. Wang, P. Hu, Perspective: Photocatalytic reduction of CO_2 to solar fuels over semiconductors, J. Chem. Phys., 147 (2017) 030901.
[6] H. Zhao, F. Pan, Y. Li, A review on the effects of TiO_2 surface point defects on CO_2 photoreduction with H_2O, Journal of Materiomics, 3 (2017) 17-32.
[7] C. Song, Global Challenges and Strategies for Control, Conversion and Utilization of CO_2 for Sustainable Development Involving Energy, Catalysis, Adsorption and Chemical Processing, Cat. Today 115 (2006) 2-32.
[8] S.C. Roy, O.K. Varghese, M. Paulose, C.A. Grimes, Toward solar fuels: photocatalytic conversion of carbon dioxide to hydrocarbons, ACS Nano, 4 (2010) 1259-1278.
[9] M. Mikkelsen, M. Jorgensen, F.C. Krebs, The teraton challenge. A review of fixation and transformation of carbon dioxide, Energy Environ Sci., 3 (2010) 43-81.
[10] S.N. Habisreutinger, L. Schmidt-Mende, J.K. Stolarczyk, Photocatalytic Reduction of CO_2 on TiO_2 and Other Semiconductors, Angew. Chem. Int. Ed., 52 (2013) 7372-7408.

[11] A. Goeppert, M. Czaun, J.-P. Jones, G.K. Surya Prakash, G.A. Olah, Recycling of carbon dioxide to methanol and derived products - closing the loop, Chem. Soc. Rev., 43 (2014) 7995-8048.
[12] O.K. Varghese, M. Paulose, T.J. LaTempa, C.A. Grimes, High-Rate Solar Photocatalytic Conversion of CO_2 and Water Vapor to Hydrocarbon Fuels, Nano Lett., 9 (2009) 731-737.
[13] O.K. Varghese, M. Paulose, T.J. LaTempa, C.A. Grimes, High-Rate Solar Photocatalytic Conversion of CO_2 and Water Vapor to Hydrocarbon Fuels, Nano Lett., 10 (2010) 750-750.
[14] A.K. Mishra, A. Roldán, N.H.d. Leeuw, A density functional theory study of the adsorption behaviour of CO_2 on Cu_2O surfaces, J. Chem. Phys., 145 (2016) 044709.
[15] A.A. Peterson, F. Abild-Pedersen, F. Studt, J. Rossmeisl, J.K. Nørskov, How copper catalyzes the electroreduction of carbon dioxide into hydrocarbon fuels, Energy Environ Sci., 3 (2010) 1311-1315.
[16] E.L. Uzunova, N. Seriani, H. Mikosch, CO_2 conversion to methanol on Cu(I) oxide nanolayers and clusters: an electronic structure insight into the reaction mechanism, Phys. Chem. Chem. Phys., 17 (2015) 11088-11094.
[17] H. Wu, N. Zhang, H. Wang, S. Hong, Adsorption of CO_2 on Cu_2O (111) oxygen-vacancy surface: First-principles study, Chem. Phys. Lett., 568 (2013) 84-89.
[18] L.I. Bendavid, E.A. Carter, CO_2 Adsorption on Cu_2O(111): A DFT+U and DFT-D Study, J. Phys. Chem. C, 117 (2013) 26048-26059.
[19] H. Wu, N. Zhang, H. Wang, S. Hong, Adsorption of CO_2 on Cu_2O (111) oxygen-vacancy surface: First-principles study, Chem. Phys. Lett., 568-569 (2013) 84-89.
[20] L. Liu, C. Zhao, Y. Li, Spontaneous Dissociation of CO_2 to CO on Defective Surface of Cu(I)/TiO_{2-x} Nanoparticles at Room Temperature, J. Phys. Chem. C, 116 (2012) 7904-7912.
[21] H. Wu, N. Zhang, Z. Cao, H. Wang, S. Hong, The adsorption of CO_2, H_2CO_3, HCO_3^- and CO_3^{2-} on Cu_2O (111) surface: First-principles study, Int. J. Quantum Chem, 112 (2012) 2532-2540.
[22] D. Gao, I. Zegkinoglou, N.J. Divins, F. Scholten, I. Sinev, P. Grosse, B. Roldan Cuenya, Plasma-Activated Copper Nanocube Catalysts for Efficient Carbon Dioxide Electroreduction to Hydrocarbons and Alcohols, ACS Nano, 11 (2017) 4825-4831.
[23] H. Mistry, A.S. Varela, C.S. Bonifacio, I. Zegkinoglou, I. Sinev, Y.-W. Choi, K. Kisslinger, E.A. Stach, J.C. Yang, P. Strasser, B.Roldan Cuenya, Highly selective plasma-activated copper catalysts for carbon dioxide reduction to ethylene, Nature Communications, 7 (2016) 12123.
[24] M. Favaro, H. Xiao, T. Cheng, W.A. Goddard, J. Yano, E.J. Crumlin, Subsurface oxide plays a critical role in CO_2 activation by Cu(111) surfaces to form chemisorbed CO_2, the first step in reduction of CO_2 , Proceedings of the National Academy of Sciences, 114 (2017) 6706-6711.
[25] L. Wang, K. Gupta, J.B.M. Goodall, J.A. Darr, K.B. Holt, In situ spectroscopic monitoring of CO2 reduction at copper oxide electrode, Faraday Discuss., 197 (2017) 517-532.
[26] S.A. Akhade, W. Luo, X. Nie, A. Asthagiri, M.J. Janik, Theoretical insight on reactivity trends in CO2 electroreduction across transition metals, Catal. Sci. Technol., 6 (2016) 1042-1053.
[27] V.P. Indrakanti, Photoinduced activation of CO_2 on TiO_2 surfaces: Quantum chemical modeling of CO_2 adsorption on oxygen vacancies, Fuel Process. Technol., 92 (2011) 805-811
[28] W. Pipornpong, R. Wanbayor, V. Ruangpornvisuti, Adsorption of CO_2 on the perfect and oxygen vacancy defect surfaces of anatase TiO_2 and its photocatalytic mechanism of conversion to CO, Appl. Surf. Sci., 257 (2011) 10322-10328.
[29] D. Lee, Y. Kanai, Role of Four-Fold Coordinated Titanium and Quantum Confinement in CO_2 Reduction at Titania Surface, J. Am. Chem. Soc., 134 (2012) 20266-20269.
[30] U. Tumuluri, J.D. Howe, W.P. Mounfield, M. Li, M. Chi, Z.D. Hood, K.S. Walton, D.S. Sholl, S. Dai, Z. Wu, Effect of Surface Structure of TiO_2 Nanoparticles on CO_2 Adsorption and SO_2 Resistance, ACS Sustainable Chemistry & Engineering, 5 (2017) 9295-9306.
[31] X. Lin, Z.-T. Wang, I. Lyubinetsky, B.D. Kay, Z. Dohnalek, Interaction of CO_2 with oxygen adatoms on rutile TiO_2(110), Phys. Chem. Chem. Phys., 15 (2013) 6190-6195.
[32] X. Lin, Y. Yoon, N.G. Petrik, Z. Li, Z.-T. Wang, V.-A. Glezakou, B.D. Kay, I. Lyubinetsky, G.A. Kimmel, R. Rousseau, Z. Dohnálek, Structure and Dynamics of CO_2 on Rutile TiO_2(110)-1×1, J. Phys. Chem. C, 116 (2012) 26322-26334.

[33] W.-J. Yin, B. Wen, S. Bandaru, M. Krack, M.W. Lau, L.-M. Liu, The Effect of Excess Electron and hole on CO_2 Adsorption and Activation on Rutile (110) surface, Scientific Reports, 6 (2016) 23298.
[34] C.-T. Yang, B.C. Wood, V.R. Bhethanabotla, B. Joseph, CO_2 Adsorption on Anatase TiO_2 (101) Surfaces in the Presence of Subnanometer Ag/Pt Clusters: Implications for CO_2 Photoreduction, J. Phys. Chem. C, 118 (2014) 26236-26248.
[35] J. Graciani, K. Mudiyanselage, F. Xu, A.E. Baber, J. Evans, S.D. Senanayake, D.J. Stacchiola, P. Liu, J. Hrbek, J.F. Sanz, J.A. Rodriguez, Highly active copper-ceria and copper-ceria-titania catalysts for methanol synthesis from CO_2, Science, 345 (2014) 546-550.
[36] M. Behrens, F. Studt, I. Kasatkin, S. Kühl, M. Hävecker, F. Abild-Pedersen, S. Zander, F. Girgsdies, P. Kurr, B.-L. Kniep, M. Tovar, R.W. Fischer, J.K. Nørskov, R. Schlögl, The Active Site of Methanol Synthesis over $Cu/ZnO/Al_2O_3$ Industrial Catalysts, Science, 336 (2012) 893-897.
[37] Y. Wang, J. Zhao, T. Wang, Y. Li, X. Li, J. Yin, C. Wang, CO_2 photoreduction with H_2O vapor on highly dispersed CeO_2/TiO_2 catalysts: Surface species and their reactivity, J. Catal., 337 (2016) 293-302.
[38] M. Fronzi, W. Daly, M. Nolan, Reactivity of metal oxide nanocluster modified rutile and anatase TiO_2: Oxygen vacancy formation and CO_2 interaction, Applied Catalysis A: , 521 (2016) 240-249.
[39] M. Nolan, A. Iwaszuk, A.K. Lucid, J.J. Carey, M. Fronzi, Design of novel visible light active photocatalyst materials: surface modified TiO_2, Adv. Mater., 28 (2016) 5425-5446.
[40] M. Fronzi, A. Iwaszuk, A. Lucid, M. Nolan, Metal oxide nanocluster-modified TiO_2 as solar activated photocatalyst materials, J. Phys.: Condens. Matter, 28 (2016) 074006.
[41] H. Tada, Q. Jin, A. Iwaszuk, M. Nolan, Molecular-scale transition metal oxide nanocluster surface-modified titanium dioxide as solar-activated environmental catalysts, J. Phys. Chem. C, 118 (2014) 12077-12086.
[42] A. Iwaszuk, A.K. Lucid, K.M. Razeeb, M. Nolan, First principles investigation of anion-controlled red shift in light absorption in ZnX (X = O, S, Se) nanocluster modified rutile TiO_2, J. Mater. Chem. A, 2 (2014) 18796-18805.
[43] A. Iwaszuk, M. Nolan, SnO-nanocluster modified anatase TiO_2 photocatalyst: exploiting the Sn(II) lone pair for a new photocatalyst material with visible light absorption and charge carrier separation, J. Mater. Chem. A, 1 (2013) 6670-6677.
[44] A. Iwaszuk, M. Nolan, Q. Jin, M. Fujishima, H. Tada, Origin of the Visible-Light Response of Nickel(II) Oxide Cluster Surface Modified Titanium(IV) Dioxide, J. Phys. Chem. C, 117 (2013) 2709-2718.
[45] Q. Jin, M. Fujishima, A. Iwaszuk, M. Nolan, H. Tada, Loading Effect in Copper(II) Oxide Cluster-Surface-Modified Titanium(IV) Oxide on Visible- and UV-Light Activities, J. Phys. Chem. C, 117 (2013) 23848-23857.
[46] Q. Jin, M. Fujishima, M. Nolan, A. Iwaszuk, H. Tada, Photocatalytic activities of tin(IV) oxide surface-modified titanium(IV) dioxide show a strong sensitivity to the TiO_2 crystal form, J. Phys. Chem. C, 116 (2012) 12621-12626.
[47] M. Nolan, First-Principles Prediction of New Photocatalyst Materials with Visible-Light Absorption and Improved Charge Separation: Surface Modification of Rutile TiO_2 with Nanoclusters of MgO and Ga_2O_3, ACS Appl. Mater. Interfaces, 4 (2012) 5863-5871.
[48] A. Iwaszuk, M. Nolan, Reactivity of sub 1 nm supported clusters: $(TiO_2)_n$ clusters supported on rutile TiO_2 (110), Phys. Chem. Chem. Phys., 13 (2011) 4963-4973.
[49] M. Nolan, Electronic coupling in iron oxide-modified TiO_2 leads to a reduced band gap and charge separation for visible light active photocatalysis, Phys. Chem. Chem. Phys., 13 (2011) 18194-18199.
[50] S. Rhatigan, M. Nolan, Impact of surface hydroxylation in MgO-/SnO-nanocluster modified TiO_2 anatase (101) composites on visible light absorption, charge separation and reducibility, Chin. Chem. Lett., (2017) doi: 10.1016/j.cclet.2017.11.036

[51] A. Lucid, A. Iwaszuk, M. Nolan, A first principles investigation of Bi_2O_3-modified TiO_2 for visible light Activated photocatalysis: The role of TiO_2 crystal form and the Bi^{3+} stereochemical lone pair, Mater. Sci. Semicond. Process., 25 (2014) 59-67.
[52] K.C. Schwartzenberg, J.W.J. Hamilton, A.K. Lucid, E. Weitz, J. Notestein, M. Nolan, J.A. Byrne, K.A. Gray, Multifunctional photo/thermal catalysts for the reduction of carbon dioxide, Catal. Today, 280 (2017) 65-73.
[53] U. Burghaus, Surface chemistry of CO_2 – Adsorption of carbon dioxide on clean surfaces at ultrahigh vacuum, Prog. Surf. Sci., 89 (2014) 161-217.
[54] S. Funk, T. Nurkic, B. Hokkanen, U. Burghaus, CO_2 adsorption on Cr(110) and Cr_2O_3(0001)/Cr(110), Appl. Surf. Sci., 253 (2007) 7108-7114.
[55] M.W. Abee, S.C. York, D.F. Cox, CO_2 Adsorption on α-Cr_2O_3 (10$\bar{1}$2) Surfaces, J. Phys. Chem. B, 105 (2001) 7755-7761.
[56] O. Seiferth, K. Wolter, B. Dillmann, G. Klivenyi, H.J. Freund, D. Scarano, A. Zecchina, IR investigations of CO_2 adsorption on chromia surfaces: Cr_2O_3 (0001)/Cr(110) versus polycrystalline α-Cr_2O_3, Surf. Sci., 421 (1999) 176-190.
[57] H. Kuhlenbeck, C. Xu, B. Dillmann, M. Haßel, B. Adam, D. Ehrlich, S. Wohlrab, H.-J. Freund, U. A. Ditzinger, H. Neddermeyer, M. Neumann, M. Neuber., Adsorption and Reaction on Oxide Surfaces: CO and CO_2 on Cr_2O_3(111), Berichte der Bunsengesellschaft für physikalische Chemie, 96 (1992) 15-27.
[58] M. Fronzi, M. Nolan, Surface Modification of Perfect and Hydroxylated TiO_2 Rutile (110) and Anatase (101) with Chromium Oxide Nanoclusters, ACS Omega, 2 (2017) 6795-6808.
[59] G. Kresse, J. Hafner, *Ab initio* molecular dynamics for liquid metals, Phys. Rev. B., 47 (1993) 558.
[60] G. Kresse, J. Hafner, *Ab initio* molecular-dynamics simulation of the liquid-metal-amorphous-semiconductor transition in germanium, Phys. Rev. B., 49 (1994) 14251-14269.
[61] G. Kresse, J. Furthmüller, Efficiency of Ab-initio Total Energy Calculations for Metals and Semiconductors using a Plane-wave Basis Set, Computational Materials Science, 6 (1996) 15-50.
[62] G. Kresse, J. Furthmüller, Efficient Iterative Schemes for Ab-initio Total-energy Calculations using a Plane-wave Basis Set, Phys. Rev. B., 54 (1996) 11169.
[63] G. Kresse, D. Joubert, From ultrasoft pseudopotentials to the projector augmented-wave method, Phys. Rev. B., 59 (1999) 1758-1775.
[64] P.E. Blöchl, Projector augmented-wave method, Phys. Rev. B., 50 (1994) 17953-17979.
[65] J.P. Perdew, J.A. Chevary, S.H. Vosko, K.A. Jackson, M.R. Pederson, D.J. Singh, C. Fiolhais, Atoms, molecules, solids, and surfaces: Applications of the generalized gradient approximation for exchange and correlation, Phys. Rev. B., 46 (1992) 6671-6687.
[66] S. Dudarev, G. Botton, S. Savrasov, C. Humphreys, A. Sutton, Electron-Energy-Loss Spectra and the Structural Stability of Nickel Oxide: An LSDA+U study, Phys. Rev. B., 57 (1998) 1505.
[67] J.J. Carey, M. Nolan, Enhancing the oxygen vacancy formation and migration in bulk chromium(III) oxide by alkali metal doping: a change from isotropic to anisotropic oxygen diffusion, J. Mater. Chem. A, 5, (2017) 15613 – 15630.
[68] J.J. Carey, M. Legesse, M. Nolan, Low Valence Cation Doping of Bulk Cr_2O_3: Charge Compensation and Oxygen Vacancy Formation, J. Phys. Chem. C, 120 (2016) 19160-19174.
[69] S. Posada-Pérez, F. Viñes, P.J. Ramirez, A.B. Vidal, J.A. Rodriguez, F. Illas, The bending machine: CO2 activation and hydrogenation on δ-MoC(001) and β-Mo2C(001) surfaces, Phys. Chem. Chem. Phys., 16 (2014) 14912-14921.
[70] NIST, NIST Standard Reference Database Number 69, NIST, 2017.